Synthesis, Crystal Structure, and Electrical Properties of Novel Radical Cation Salts of Iodine-Substituted TTF-Derived Donors with the Nitroprusside Anion Exhibiting Strong -I···NC- Interactions

Kazumasa Ueda,*[a] Toyonari Sugimoto,[b] Christophe Faulmann,[a] and Patrick Cassoux[a]

Keywords: Cations / Radical ions / Fulvalenes / Conducting materials

Radical-cation salts of iodine-substituted TTF derivatives [diiodoethylenedithiotetrathiafulvalene (**1**) diiodoethylenedithiodiselenadithiafulvalene (**2**), or iodoethylenedithiotetrathiafulvalene (**3**)] with the $[Fe(CN)_5NO]^{2-}$ nitroprusside anion, namely, $\mathbf{1}_4$·$[Fe(CN)_5NO]$, $\mathbf{2}_4$·$[Fe(CN)_5NO]$ and $\mathbf{3}_3$·$[Fe(CN)_5NO]$, were synthesized by electrocrystallization from solutions of the appropriate TTF derivative in CH_2Cl_2 with bis(tetraphenylphosphonium)nitroprusside $[(PPh_4)_2\{Fe(CN)_5NO\}]$ as electrolyte. An X-ray structure analysis indicates that the crystal structures of $\mathbf{1}_4$·$[Fe(CN)_5NO]$ and $\mathbf{2}_4$·$[Fe(CN)_5NO]$ are very similar. In both cases, molecules **1** and **2** are stacked along the *c* direction, with their long molecular axis parallel to each other. By contrast, in $\mathbf{3}_3$·$[Fe(CN)_5NO]$, molecules **3** are stacked in triad units in which two of the molecules are arranged in a face-to-face fashion and the remaining molecule is arranged in a head-to-tail fashion with respect to its neighboring molecules. In all cases, several effective iodine-nitrogen contacts between donor molecules and $[Fe(CN)_5NO]^{2-}$ anions are observed. The room temperature electrical conductivities of $\mathbf{1}_4$·$[Fe(CN)_5NO]$, $\mathbf{2}_4$·$[Fe(CN)_5NO]$ and $\mathbf{3}_3$·$[Fe(CN)_5NO]$ are $<10^{-6}$, 2.2×10^{-2} and 5 S cm^{-1}, respectively. The temperature dependence of the electrical conductivity of $\mathbf{3}_3$·$[Fe(CN)_5NO]$ reveals semiconducting behavior with a small activation energy of 30 meV. The temperature dependence of the electrical conductivity of $\mathbf{2}_4$·$[Fe(CN)_5NO]$ also reveals a semiconducting behavior, but with two regimes: above 200 K the activation energy is 60 meV and becomes much smaller — 0.2 meV — below this temperature.

Introduction

Much current research is directed toward the formation of new molecular materials in which electrical conductivity coexists with other physical phenomena. One of the recent trends in this area is the combination of conducting and optical properties. In this area, the $[Fe(CN)_5NO]^{2-}$ anion ($[NP]^{2-}$) is of highest interest because it possesses extremely long-lived metastable states at low temperature that can be generated by laser irradiation.[1−6] It has been proposed that this electronic transition might be accompanied by possible changes in the geometry of the complex anion.[5] These changes may, in turn, affect the conducting properties of derived radical salts of organic donor molecules. In this context, the use of the $[NP]^{2-}$ anion and related transition metal mononitrosyl counteranions in radical cation salts of TTF- and TSF-derived donors (TTF = tetrathiafulvalene; TSF = tetraselenafulvalene) has been contemplated.[7−10] The existence of metastable states has indeed been detected in $(BEDT\text{-}TTF)_4$·$K[NP]_2$ [BEDT-TTF = bis(ethylenedithio)tetrathiafulvalene] and $(TTF)_7[NP]_2$ by DSC measurements,[10] but no effect of the above-mentioned changes of the geometry of the $[NP]^{2-}$ anion on the conducting behavior of these radical-cation salts has yet been observed. One, possibly more effective, approach for constructing novel photochromic organic conductors might consist of introducing a strong interaction between the donor molecules and the counteranions. In such systems, the changes in geometry of the excited states of the counteranions could affect the conducting properties more efficiently through stronger intermolecular interactions.

On the other hand, promoting a stronger interaction between the organic donor and the inorganic counteranions of radical salts is being investigated more and more for ensuring a better control of the molecular arrangement of these salts.[11−17] For example, radical salts of iodine-substituted TTF-derived donors such as diiodoethylenedithiotetrathiafulvalene (**1**) diiodoethylenedithiodiselenadithiafulvalene (**2**), or iodoethylenedithiotetrathiafulvalene (**3**) with cyano-group-containing anions such as $Ag[(CN)_2]^-$, $Pd[(CN)_4]^{2-}$, or with the $[Pd(mnt)_2]^{2-}$ anion (mnt = maleonitriledithiolate), have been synthesized and their crystal structures examined.[15−17] A PM3 MO calculation of **3** indicates a HOMO extended to the iodine atom. The largest

[a] Equipe Précurseurs Moléculaires et Matériaux, LCC/CNRS
205 route de Narbonne, 31077 Toulouse Cedex 04, France
Fax: (internat.) + 33-5/61553003
[b] Research Institute for Advanced Science and Technology, Osaka Prefecture University
Sakai, Osaka 599-8570, Japan
Fax: (internat.) + 81-722/54-9935
E-mail: kazueda@riast.osakafu-u.ac.jp

coefficient of the lowest unoccupied molecular orbital (LUMO) on the iodine atom suggests that it would be the driving force of the strong interactions with the cyano group. Extremely short I···N distances in the crystal structure of $\mathbf{3}_3$·[$Ag(CN)_4$], which are almost 20% shorter than the sum of the van der Waals radii (3.53 Å), arise from an interaction between the lone pair on the nitrogen atom and the p_π LUMO on the iodine atom.[15] In the crystal structure of $\mathbf{2}_4$·[$Pd(CN)_4$], reticulated donor···anion contacts were constructed using the strong and directional -I···NC- interaction.[16]

Combining both strategies, it was hoped that radical-cation salts of iodine-substituted organic donors and the $[NP]^{2-}$ anion could be organic conductors in which the existence of metastable states in the $[NP]^{2-}$ anion could affect the electrical conducting properties via possibly strong -I···NC- interaction.

Herein we report the synthesis, crystal structure and electrical conducting properties of novel radical-cation salts formed from the iodine-substituted donor molecules **1**, **2** and **3**, and the $[NP]^{2-}$ anion.

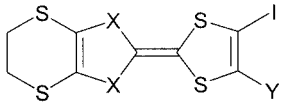

1: X = S, Y = I; **2**: X = Se, Y = I; **3**: X = S, Y = H

Results and Discussion

Synthesis

The iodine-substituted TTF-derived donors **1** and **3** were synthesized in accordance with the literature.[19] Compound **2** was synthesized by a modification of the method used for the preparation of **1** (see Exp. Sect.).

The salts $\mathbf{1}_4$·[$Fe(CN)_5NO$], $\mathbf{2}_4$·[$Fe(CN)_5NO$] and $\mathbf{3}_3$·[$Fe(CN)_5NO$], were synthesized by electro-crystallization from solutions of the appropriate iodine-substituted TTF-derived donors in CH_2Cl_2 with bis(tetraphenylphosphonium)nitroprusside [$(PPh_4)_2$·{$Fe(CN)_5NO$}] as electrolyte.

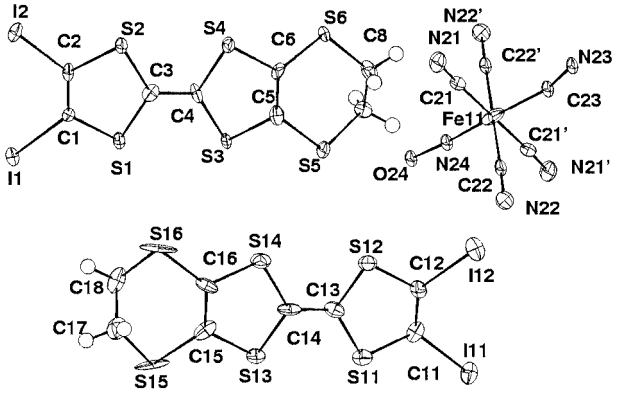

Figure 1. Atomic numbering scheme for $\mathbf{1}_4$·[NP]

Crystal Structures

1_4·[NP] and 2_4·[NP]

These two compounds are isostructural. The asymmetric unit (Figure 1 and 2) contains two donor molecules and half an [NP] entity, with the Fe atom lying on a center of inversion.

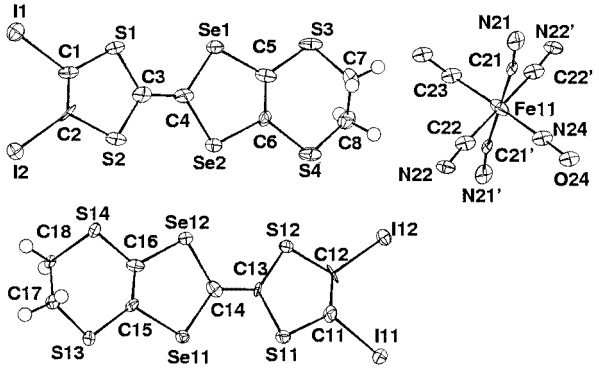

Figure 2. Atomic numbering scheme for $\mathbf{2}_4$·[NP]

Figure 3a and 3b show projections of the crystal structures of $\mathbf{1}_4$·[NP] and $\mathbf{2}_4$·[NP] down the *ab* plane. Their struc-

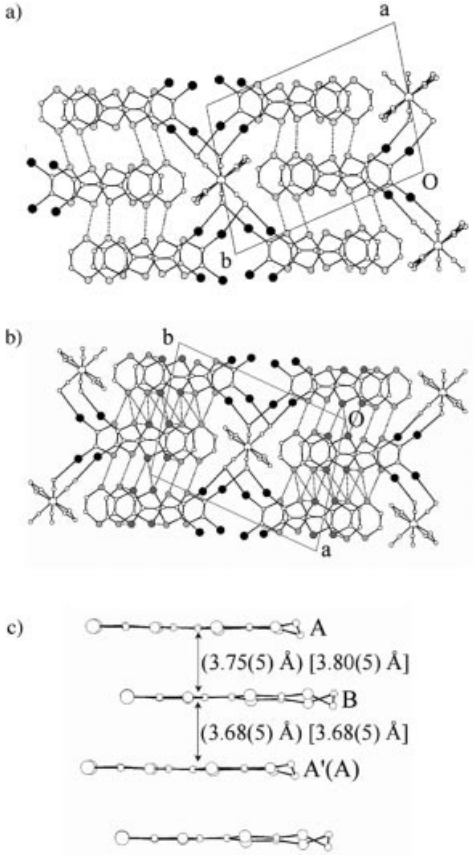

Figure 3. Projection down the *ab* plane for $\mathbf{1}_4$·[NP] (a) and $\mathbf{2}_4$·[NP] (b) and projection down the *bc* plane for both compounds (c). In Figure 3a and 3b, iodine, sulfur and selenium atoms are depicted with filled, light grey and dark grey circles, respectively. Thin dotted and solid lines show chalcogen-chalcogen and iodine-nitrogen intermolecular contacts, respectively

tures consist of sheets of adjacent columns of donor molecules in the *ac* plane alternating with layer of anions along the *b* direction (Figure 3a and 3b). The donor molecules stack along the *c* direction, with their long molecular axis parallel to each other (Figure 3c). The inter-planar distances are 3.78(3) and 3.65(3) Å for $\mathbf{1}_4$·[NP], and 3.72(5) and 3.76(5) Å for $\mathbf{2}_4$·[NP] i.e., rather longer than the "π-cloud thickness".[18]

Since the $[NP]^{2-}$ ions are located at a center of symmetry, there is a positional disorder in the NO^+ and CN^- ligands. Two kinds of overlapping mode [**A/B** and **B/A′(A)**] are observed in $\mathbf{1}_4$·[NP], as shown in Figure 4, as well as in $\mathbf{2}_4$·[NP] (not shown).

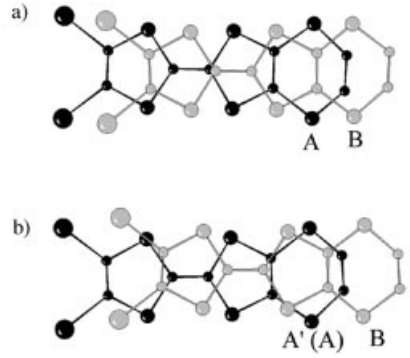

Figure 4. Modes of overlap of molecules **1** in $\mathbf{1}_4$·[NP]: (a) **A** and **B**, and (b) **B** and **A′(A)**

In both overlapping modes one molecule is stacked over the other molecule with a ring-over-bond type mode, since the molecules are slipped along their long axis.

Moreover, in $\mathbf{1}_4$·[NP], some effective side-by-side contacts are observed between donor molecules of adjacent columns. Indeed, interatomic distances rather shorter than the sum of the van der Waal's radii (3.70 Å) are observed between sulfur atoms of the ethylenedithio group and of the TTF moiety [S6···S11: 3.497(6); S2···S15: 3.536(6); S1···S16: 3.541(7); S14···S16: 3.601(8); S1···S5: 3.632(7) Å].

Even more importantly, several short contacts between the donor **1** and the $[NP]^{2-}$ anion through -I···NC- contacts are also observed, as indicated by several interatomic distances between iodine atoms of **1** and nitrogen atoms of the $[NP]^{2-}$ anion [I1···N22: 3.08(2); I2···N21: 3.11(1); I11···N22: 3.08(1); I12···N21: 3.25(2) Å], which are shorter than the sum (3.53 Å) of the van der Waals radii of the iodine and nitrogen atoms.

Due to the presence of Se atoms, $\mathbf{2}_4$·[NP] exhibits more contacts than $\mathbf{1}_4$·[NP]. The interaction between adjacent columns is accomplished through contacts between different sulfur atoms [S1···S1: 3.70(1); S2···S14: 3.59(1); S3···S11: 3.67(1); S4···S12: 3.55(1) and S11···S13: 3.66(1) Å], as well as between sulfur and selenium atoms [Se1···S3: 3.58(1) Å] and different selenium atoms [Se1···Se11: 3.67(1); Se2···Se2: 3.83(1); Se2···Se12: 3.67(1) and Se11···Se11: 3.77(1) Å], shorter than the sum of the corresponding van der Waals radii of the corresponding chalcogen atoms (3.70 Å for S···S, 3.80 Å for S···Se, and 3.90 for Se···Se). In addition, as for $\mathbf{1}_4$·[NP], several short interatomic distances [I1···N22: 3.25(3); I2···N21: 3.07(3); I11···N21: 3.07(3); I12···N22: 3.10(2) Å] are observed between the iodine atoms of **2** and nitrogen atoms of the $[NP]^{2-}$ anion.

$\mathbf{3}_3$·[NP]

The asymmetric unit (Figure 5) of $\mathbf{3}_3$·[NP] contains half an [NP] entity, with the Fe atom lying on a center of inversion, and two molecules of the donor **3**, among which one of the donor molecules (the one containing I11) has an occupancy of one half, since it is placed close to an inversion center.

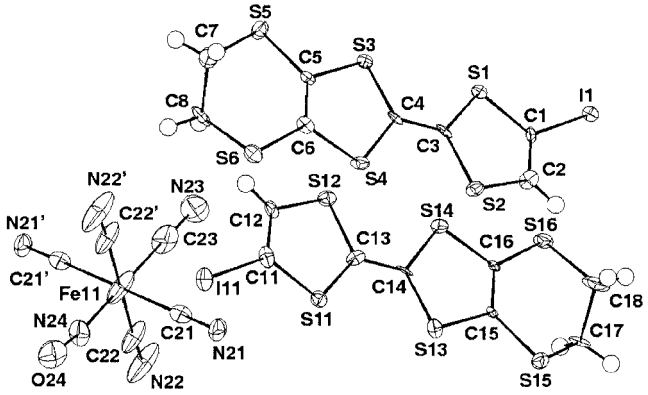

Figure 5. Atomic numbering scheme for $\mathbf{3}_3$·[NP]

Figure 6a and 6b shows the projections of the crystal structure down to the *bc* and *ab* planes. The structure consists of sheets of columns of **3** in the *ac* plane alternating with layers of $[NP]^{2-}$ anions along the *b* direction.

As shown in Figure 6b and 6c, the donor molecules **3** are stacked in a triad arrangement, ···**ABAABA**···. A **B** molecule is close to the center of symmetry, depicted as the gray circle, resulting in two orientations of the **B** molecule (**B** and **B′** generated by a symmetry operation of **B**) within a triad. Because of these two orientations of **B** molecules within the triad, there are two kinds of stacking mode: one of type **I** (shown at the top of Figure 6b and 6c), and the other of type **II** (shown at the bottom of Figure 6b and 6c). In the triad unit, two of the three molecules **3** (**A** and **B**) (type **I**), or **B′** and **A′′′** (type **II**) are arranged in a face-to-face fashion, whereas the remaining molecule (**A′** in type **I** and **A′′** in type **II**) is arranged in a head-to-tail fashion with respect to the **B** molecule (type **I**) or **B′** (type **II**). The inter-planar distances are 3.63(5) Å between the face-to-face molecules and 3.57(5) Å between the head-to-tail ones. The inter-planar distances are slightly longer than the "π-cloud thickness" (3.50 Å), but the [**A′/A"**] inter-planar distance between the triads is rather shorter [3.07(5) Å]. Figure 7a shows the overlap between the face-to-face molecules (**A** and **B** in mode **I**, or **B′** and **A′′′** in mode **II**). In this mode, **A** and **B** molecules are slipped transversally, resulting in a partial overlap of both molecules, but without any short S···S contacts.

In the head-to-tail mode (Figure 7b and **B/A′** or **A′′/B′** in Figure 6b and 6c), the molecules are slipped longitudinally,

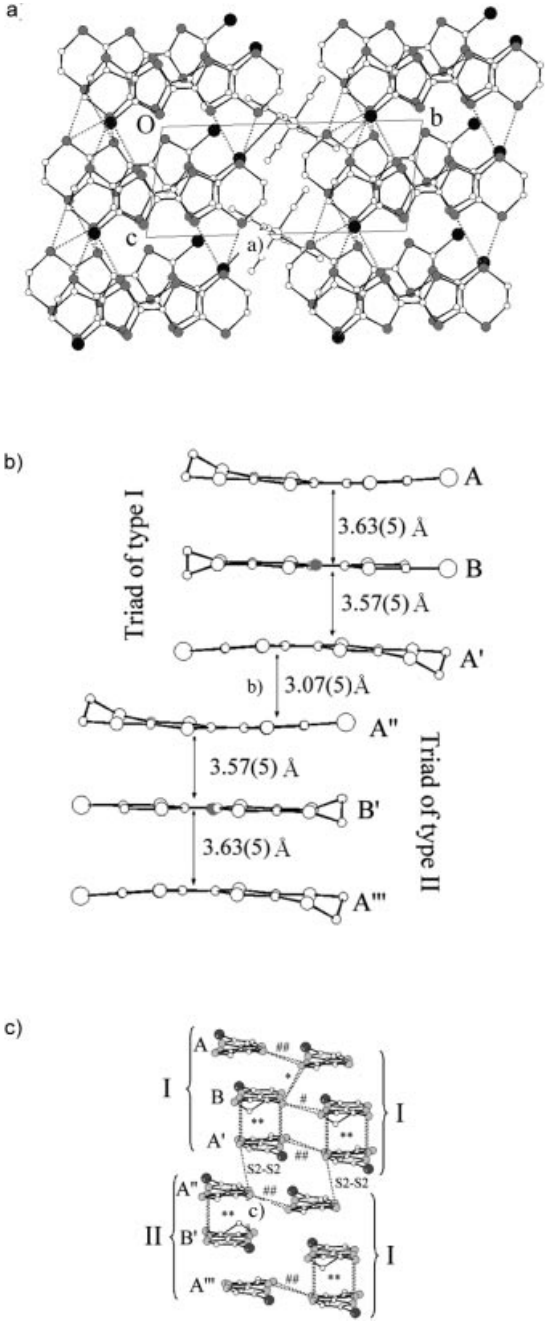

Figure 6. (a): Projection down the *bc* plane of $\mathbf{3}_3$·[NP]. Iodine and sulfur atoms are depicted with filled and grey circles, respectively. Dotted and solid lines show sulfur-sulfur and iodine-nitrogen contacts, respectively. (b): Projection down the *ab* plane showing the stacking modes of type **I** and **II** (the center of inversion is depicted as the grey circle). (c): Projection down the *ac* plane showing the S···S contacts between triads of type **I** and **II** (see text for the meaning of the symbols)

resulting in a ring-over-bond type overlap between these molecules. This configuration leads to several S···S contacts, depicted with the symbol ** in Figure 6c [S1···S14: 3.650(7); S2···S13: 3.43(3); S3···S12: 3.489(7) and S4···S11: 3.586(8) Å]. By contrast, the overlap between **A**′ and **A**′′ molecules belonging to different triads is minimal (one sulfur atom over a dithiacyclopentene ring; Figure 7c). **A**′ and **A**′′ are connected through one contact between the S2 atoms

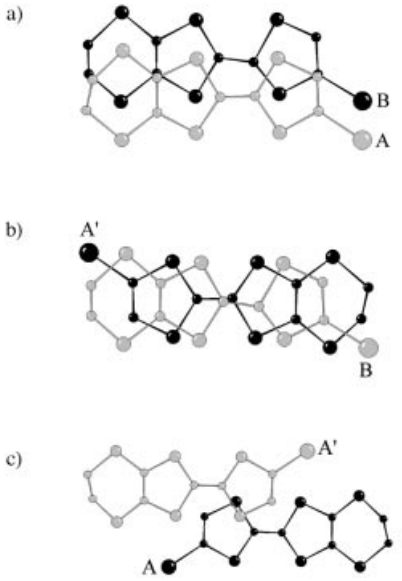

Figure 7. Modes of overlap in $\mathbf{3}_3$·[NP] between **A**/**B** (a), **B**/**A**′ (b), and **A**′/**A**′′ (c)

[3.502(4) Å]. Effective side-by-side contacts between sulfur atoms of adjacent triads are observed between **A** molecules [symbol ## in Figure 6c: S3···S6: 3.566(4); S5···S6: 3.427(5) Å], between **A** and **B** molecules [symbol * in Figure 6c: S3···S16: 3.551(7); S5···S16: 3.677(8) Å], and between **B** molecules when the adjacent triad is of the same nature [symbol # in Figure 6c: S13···S16: 3.49(1) and S15···S16: 3.37(1) Å]. Also, effective contacts between donor molecules and $[NP]^{2-}$ anions are observed, as indicated by short interatomic distances between the iodine atom of molecule **3** and nitrogen atoms of the $[NP]^{2-}$ anion [N21···I1: 2.93(1) and N22···I11: 3.51(2) Å].

In these three obtained salts, the I···N distances between the donor molecules and $[NP]^{2-}$ counterion are 8−18% shorter than the sum of the van der Waals radii of iodine and nitrogen atoms. These values indicate the existence of a strong interaction between the iodine atom of the donor molecules and a cyano group of the $[NP]^{2-}$ counterion. This strong interaction arises from an interaction between the lone pair on the nitrogen atom and the σ_p-LUMO on the iodine atom as is seen in the crystals of $\mathbf{3}_2$·$[Ag(CN)_2]$ and $\mathbf{2}_4$·$[Pd(CN)_4]$.[15,16]

Electrical Conductivity

The electrical conductivities of $\mathbf{1}_4$·[NP], $\mathbf{2}_4$·[NP] and $\mathbf{3}_3$·[NP] at room temperature are $<10^{-6}$, 2.2×10^{-2} and 5 S cm^{-1}, respectively. It should be noted that, although the structures of $\mathbf{2}_4$·[NP] and $\mathbf{1}_4$·[NP] are similar, the conductivity value determined for $\mathbf{2}_4$·[NP] is 10^4 times larger than that determined for $\mathbf{1}_4$·[NP]. This difference is likely to be due to the larger van der Waals radius of the selenium atom (2.00 Å), compared to that of the sulfur atom (1.85 Å), which induces interactions within the stack of $\mathbf{2}_4$·[NP] that are not observed in $\mathbf{1}_4$·[NP].

The temperature dependence of the resistivity was measured for $\mathbf{2}_4$·[NP] and $\mathbf{3}_3$·[NP] (Figure 8). In both cases the

resistivity increases with decreasing temperatures, indicating a semiconducting behavior. In the case of $\mathbf{3}_3$·[NP], a small activation energy of 30 meV could be determined over the entire range (300−50 K) of temperatures. In contrast, two regimes are observed for $\mathbf{2}_4$·[NP]: from 293 K down to around 200 K the activation energy is 60 meV, and below 200 K a much smaller activation energy of 0.2 meV is found. The electrical conducting properties of these three salts can be readily understood by considering their crystal structures. The interplanar distances of **1** and **2** molecules in their columns are rather longer than the "π-cloud thickness". This means that the large interplanar distances between molecules suppress an effective overlap of the π-orbital of the donor molecules along the stacking direction. As a result of this unfavorable π-orbital interaction, these two salts have comparably low conducting behaviors. On the other hand, the semiconducting property of $\mathbf{3}_3$·[NP] can be reasonably understood by considering that the column structure is triadic and not uniform.

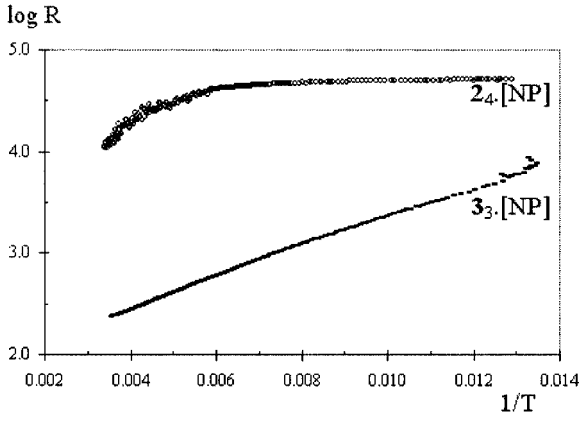

Figure 8. Temperature dependence of the resistance of single crystals of $\mathbf{2}_4$·[NP] (°) and $\mathbf{3}_3$·[NP] (−)

Conclusion

The synthesis, crystal structures and electrical conductivities of three new radical salts $\mathbf{1}_4$·[NP], $\mathbf{2}_4$·[NP] and $\mathbf{3}_3$·[NP] have been described. Both $\mathbf{2}_4$·[NP] and $\mathbf{3}_3$·[NP] are semiconductors, but two regimes, with a very low activation energy at low temperatures, are observed only for $\mathbf{2}_4$·[NP]. Although the structures of $\mathbf{2}_4$·[NP] and $\mathbf{1}_4$·[NP] are very similar, the only-sulfur containing $\mathbf{1}_4$·[NP] is an insulator with a room-temperature conductivity 10^4 times smaller than that of the sulfur-selenium containing $\mathbf{2}_4$·[NP].

The strategy of using iodine-substituted organic donors for promoting stronger donor-counteranion interaction actually led in the three salts studied here to effective contacts between the donor molecules and the $[NP]^{2-}$ anions. This is the first example in which donor molecules are connected with $[NP]^{2-}$ anions through strong and directional interactions of the -I···NC- type.

The detection of long-lived metastable states at low temperature generated by laser irradiation and conductivity measurements under irradiation remain to be carried out and are under progress.

Experimental Section

General Remarks: ^{1}H NMR spectra were recorded in $CDCl_3$ on a Bruker AC200 spectrometer. Chemical shifts are quoted relative to the residual solvent peak ($CDCl_3$: δ = 7.26 ppm). Mass spectra were recorded on a NERMAG R10-10 mass spectrometer operating in the DCI mode.

Synthesis of 2: Compound **2** was synthesized by a modification of the method used for the preparation of **1**.[19] A solution of 4,5-ethylenedithio-1,3-diselenol-2-one (217.9 mg, 0.7212 mmol) and 4,5-diiodo-2-thioxo-1,3-dithiole (556.8 mg) in toluene (20 mL) containing freshly distilled $P(OEt)_3$ (2.7 mL) was refluxed for 6 h. After removal of the solvent under reduced pressure a dark brown residue was obtained. This residue was purified by chromatography on silica gel using carbon disulfide (CS_2) as eluent to afford **2** (33.9 mg, 72% yield) which was recrystallized from CS_2/hexane. M.p. 173 °C. MS (DCI/NH_3): m/z = 643 [M^+] ^{1}H NMR ($CDCl_3/CS_2$): δ = 3.31 ppm.

Electrocrystallization of $\mathbf{1}_4$·[NP], $\mathbf{2}_4$·[NP] and $\mathbf{3}_3$·[NP]: Single crystals of $\mathbf{1}_4$·[NP], $\mathbf{2}_4$·[NP] and $\mathbf{3}_3$·[NP] were prepared by galvanostatic oxidation of the donor molecules (7.2 mg of **1** for $\mathbf{1}_4$·[NP], 9.1 mg of **2** for $\mathbf{2}_4$·[NP] and 3.8 mg of **3** for $\mathbf{3}_3$·[NP]) with $(Ph_4P)_2$[NP] (62 mg for $\mathbf{1}_4$·[NP] and $\mathbf{2}_4$·[NP], and 40 mg for $\mathbf{3}_3$·[NP]) as supporting electrolyte in CH_2Cl_2 (20 mL) under an argon atmosphere at 25 °C. A standard H-shaped cell and platinum-wire electrodes (1 mm diameter) were employed for the preparation of single crystals, applying constant currents (0.6 μA mg for $\mathbf{1}_4$·[NP] and $\mathbf{2}_4$·[NP], and 0.2 μA for $\mathbf{3}_3$·[NP]). Crystals were formed in the anode compartment, collected and washed with CH_2Cl_2: orange platelet-shaped crystals for $\mathbf{1}_4$·[NP], brown platelet-shaped crystals for $\mathbf{2}_4$·[NP], and black needle-shaped crystals for $\mathbf{3}_3$·[NP]. The composition of $\mathbf{1}_4$·[NP], $\mathbf{2}_4$·[NP] and $\mathbf{3}_3$·[NP] was determined by X-ray structure analyses.

X-ray Crystallographic Study: The X-ray diffraction data were collected at 180 K for $\mathbf{1}_4$·[NP] and $\mathbf{2}_4$·[NP], and 160 K for $\mathbf{3}_3$·[NP] on a STOE imaging plate diffractometer with graphite monochromated Mo-K_α radiation (λ= 0.71069 Å). Crystallographic data are gathered in Table 1.

The structures were solved by direct methods (SHELXS 97)[20] and refined on F_0^2 with full-matrix least-squares analysis. The calculations were carried out with the CRYSTALS[21] and WINGX[22] package programs running on a PC. For $\mathbf{1}_4$·[NP], the final cycle of least-squares refinement on F_0^2 for 5771 data and 367 parameters converged to $wR^2(F_0^2)$ = 0.231 for all data and to R = 0.075 for 3117 data with $I \geq 2\sigma(I)$. For $\mathbf{2}_4$·[NP], the final cycle of least-squares refinement on F_o^2 for 5888 data and 358 parameters converged to $wR^2(F_0^2)$ = 0.237 for all data and to R = 0.090 for 1915 data with $I \geq 2\sigma$ (I). For $\mathbf{3}_3$·[NP], the final cycle of least-squares refinement on F_o^2 for 3948 data and 349 parameters converged to $wR^2(F_0^2)$ = 0.181 for all data and to R = 0.072 for 3420 data with $I \geq 2\sigma(I)$. The drawings of the molecular structures were produced using CAMERON.[23] The atomic scattering factors were taken from International Tables for X-ray Crystallography.[24]

CCDC-193065−193067 ($\mathbf{1}_4$·[NP], $\mathbf{2}_4$·[NP]$\mathbf{3}_4$·[NP], respectively) contain the supplementary crystallographic data for this paper. These data can be obtained free of charge at www.ccdc.cam.ac.uk/conts/retrieving.html [or from the Cambridge Crystallographic Data Centre, 12, Union Road, Cambridge CB2 1EZ, UK; Fax: (internat.) +44-1223/336-033; E-mail: deposit@ccdc.cam.ac.uk].

Table 1. Crystal data for $\mathbf{1}_4$·[NP], $\mathbf{2}_4$·[NP] and $\mathbf{3}_3$·[NP]

	$\mathbf{1}_4$·[NP]	$\mathbf{2}_4$·[NP]	$\mathbf{3}_3$·[NP]
Empirical formula	$C_{37}H_{16}FeI_8N_6OS\mathbf{2}_4$	$C_{37}H_{16}FeI_8N_6OS_{16}Se_8$	$C_{29}H_{15}I_3FeN_6OS_{18}$
M	2401.0	2766.2	1477.1
Crystal system	Triclinic	Triclinic	Triclinic
Space group	$P\bar{1}$	$P\bar{1}$	$P\bar{1}$
a [Å]	12.7200(13)	12.7630(19)	10.9690(15)
b [Å]	17.2380(20)	17.3930(30)	15.2250(21)
c [Å]	7.4400(8)	7.4840(12)	6.6320(9)
α [°]	97.111(13)	96.531(20)	99.468(16)
β [°]	92.968(12)	92.119(18)	96.697(17)
γ [°]	102.456(13)	102.264(19)	92.149(17)
V [Å ^{3}]	1575.5(6)	1609.7(8)	1091.0(4)
Z	1	1	1
$d_{calcd.}$ [g·cm^{-1}]	2.53	2.86	2.25
$F(000)$	1121.9	1265.8	711.9
μ(Mo-K_α) [cm^{-1}]	4.994	9.151	3.368
Data collection			
Temperature [K]	180	180	160
Diffractometer	Stoe IPDS	Stoe IPDS	Stoe IPDS
Scan mode	Φ	Φ	Φ
Scan range Φ [°]	$0 < \Phi < 250$	$0 < \Phi < 250$	$0 < \Phi < 250$
No. of collected reflns.	5771	5888	3948
No. of reflns. used	3117 [$I > 2\sigma(I)$]	1915 [$I > 2\ \sigma\ (I)$]	3420 [$I > 2\ \sigma\ (I)$]
R	0.075	0.090	0.072
wR_2	0.231	0.237	0.181
No. of parameters	367	358	349

Electrical Conductivity Measurement: The electrical conductivity measurements were carried out on single crystals of $\mathbf{1}_4$·[NP], $\mathbf{2}_4$·[NP] and $\mathbf{3}_3$·[NP] using the four-probe method in the temperature range of 50−300 K. Contacts to the electrode were ensured by gold paste.

Acknowledgments

We thank D. Berail from Motolorola Company for supplying printed circuits for conductivity measurements. K. U. thanks Osaka Prefecture University for a postdoctoral grant.

[1] H. T. Woike, W. Krasser, S. Haussühl, *Z. Kristallogr.* **1989**, *188*, 139−153.
[2] T. Woike, W. Krasser, P. Bechthold, S. Haussühl, *Phys. Rev. Lett.* **1984**, *53*, 1767−1770.
[3] H. Zöllner, W. Krasser, T. Woike, *Chem. Phys. Lett.* **1989**, *161*, 497−501.
[4] T. Woike, S. Haussühl, *Solid State Commun.* **1993**, *86*, 333−337.
[5] M. R. Pressprich, M. A. White, V. Vekhlter, P. Coppens, *J. Am. Chem. Soc.* **1994**, *116*, 5233−5238.
[6] M. D. Carducci, M. R. Pressprich, P. Coppens, *J. Am. Chem. Soc.* **1997**, *119*, 2669−2678.
[7] L. Kushch, L. Buravov, V. Tkacheva, E. Yagubskii, L. Zorina, S. Khasanov, R. Shibaeva, *Synth. Met.* **1999**, *102*, 1646−1649.
[8] M. Gener, E. Canadell, S. S. Khasanov, L. V. Zorina, R. P. Shibaeva, L. A. Kushch, E. B. Yagubskii, *Solid State Commun.* **1999**, *111*, 329−333.
[9] L. V. Zorina, S. S. Khasanov, R. P. Shibaeva, M. Gener, R. Rousseau, E. Canadell, L. A. Kushch, E. B. Yagubskii, O. O. Drozdova, K. Yakushi, *J. Mater. Chem.* **2000**, *10*, 2017−2023.
[10] M. Clemente-Leon, E. Coronado, J. R. Galan-Mascaros, C. J. Gomez-Garcia, E. Canadell, *Inorg. Chem.* **2000**, *39*, 5394−5397.
[11] A. Dolbecq, M. Fourmigué, P. Batail, *Chem. Mater.* **1994**, *6*, 1413−1418.
[12] K. Heuzé, M. Fourmigué, P. Batil, E. Canadell, P. Auban-Senzier, *Chem. Eur. J.* **1999**, *5*, 2971−2976.
[13] K. Heuzé, M. Fourmigué, P. Batail, *J. Mater. Chem.* **1999**, *9*, 2373−2379.
[14] A. S. Batsanov, A. J. Moore, N. Robertson, A. Green, M. R. Bryce, J. A. K. Howard, A. E. Underhill, *J. Mater. Chem.* **1997**, *7*, 387−389.
[15] T. Imakubo, H. Sawa, R. Kato, *Synth. Met.* **1995**, *73*, 117−122.
[16] T. Imakubo, H. Sawa, R. Kato, *J. Chem. Soc., Chem. Commun.* **1995**, 1667−1668.
[17] T. Imakubo, H. Sawa, R. Kato, *Synth. Met.* **1997**, *86*, 1883−1884.
[18] A. Bondi, *J. Phys. Chem.* **1964**, *68*, 441−451.
[19] B. Domercq, T. Devic, M. Fourmigué, P. Auban-Senzier, E. Canadell, *J. Mater. Chem.* **2001**, *11*, 1570−1575.
[20] G. M. Sheldrick, *SHELX97 − Programs for Crystal Structure Analysis* (release 97−2), Intitut für Anorganische Chemie der Universtät, Tammanstrasse 4, Göttingen, Germany **1998**.
[21] D. J. Watkin, C. K. Prout, J. R. Carruthers, P. W. Betteridge, R. I. Cooper, *CRYSTALS*, issue 11, Chemical Crystallography Laboratory, University of Oxford, Oxford, England, **2002**.
[22] WINGX, Main Reference; L. J. Farrugia, *J. Appl. Crystallogr.* **1999**, *32*, 837−838.
[23] D. J. Watkin, C. K. Prout, L. J. Pearce, *CAMERON*, Chemical Crystallography Laboratory, University of Oxford, Oxford, England, **1996**.
[24] D. T. Cromer, J. T. Waber, *International Table for X-ray Crystallography*, Kynoch Press, Birmingham, **1974**, vol. 4.

Received November 27, 2003

